CLM-R238

CLM-R238

UKAEA

Report

PRESSURE DROP IN THE COOLANT SYSTEM OF A FUSION REACTOR WITH CONCENTRIC COOLING DUCTS

R. A. W. SHOCK

CULHAM LABORATORY
Abingdon Oxfordshire

1983

C/18

Available from H. M. Stationery Office

£2.00

CLM-R 238

PRESSURE DROP IN THE COOLANT SYSTEM OF A FUSION REACTOR WITH CONCENTRIC COOLING DUCTS

by

R. A. W. Shock*
Culham Laboratory, Abingdon, Oxon, OX14 3DB, U.K.
(Euratom/UKAEA Fusion Association)

ABSTRACT

Previous studies of the pressure drop and flow distribution in the helium coolant circuit of a fusion reactor power station have been extended to the concentric ducting case. The pressure drop characteristics of dividing and joining T's in the outer duct in such units have been separately measured. In this work these characteristics have been used to deduce the behaviour of rows of blanket cells, half segments and full segments. The overall pressure drops are found to be little different from those for the side-by-side case but the maldistribution is rather lower. It is shown that there are savings not only in material but also in the volume taken up by the ducting pipework.

* Engineering Sciences Division, AERE Harwell, Oxon, OX11 0RA, U.K.

March 1983

ISBN 0 85311 1227

CONTENTS

APPENDICES

TABLES

1. INTRODUCTION

This study extends an earlier examination of flow and pressure drop in a helium cooled fusion power station to the case where some, at least, of the ducts are based on a concentric geometry. Shock (1979, 1980) has carried out a parametric study of the flow circuit of a helium-cooled fusion power station. The pumping power fraction was calculated as a function of several parameters including coolant flowrate, first wall loading, coolant inlet temperature and temperature increase and material of construction; possible design envelopes were identified and one for a typical set of constraints is shown in Figure 1.

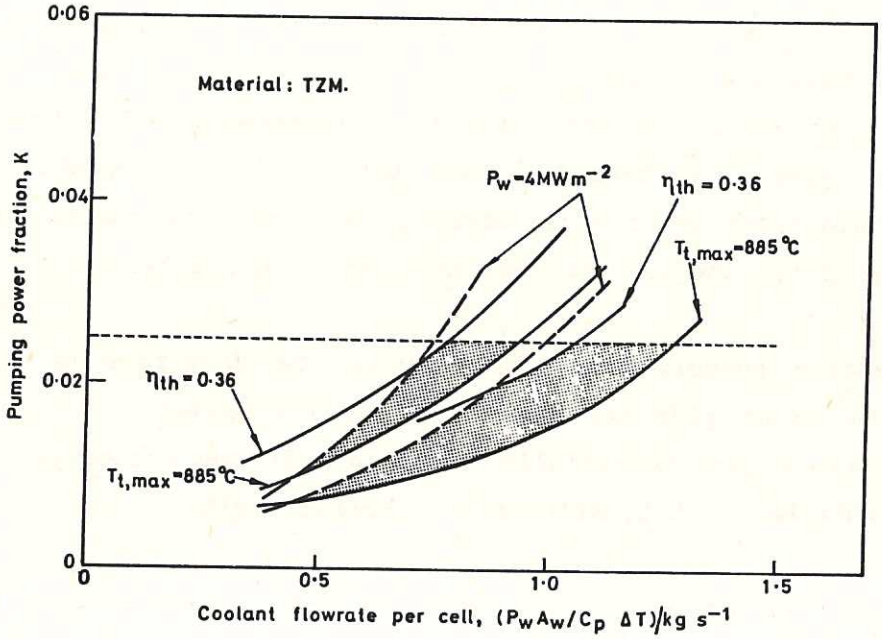

Fig.1 Design option regions. The thick curves are for p = 60 bar, d_i = 20mm, T_{in} = 200°C, the thin curves are for p = 40 bar, d_i = 25mm, T_{in} = 300°C. The dashed curves give the minimum coolant flow for 4MW m^{-2} wall loading for the two sets of conditions.

The pressure and flow distributions within the reactor were solved by considering the constituent parts (blanket cells, straight pipes, dividing and joining T's and bends), writing the pressure drop and flow conservation equations for each and solving the resulting set of non-linear simultaneous equations. The necessary equations, the solution techniques and the results are discussed by Shock (1979). The study was as general as possible but, where it was necessary to be specific about geometric parameters, these were based on Culham Conceptual Tokamak Reactor (CCTR) Mark II-A. This design is discussed in some detail by Mitchell (1978). A later design, CCTR-II-B,

differs in several respect from the former, e.g. lower power output, 1200 MW_e compared with 2500 MW_e, slightly lower size, major radius 6.7 m compared with 7.4 m and lower first wall loading, 4.5 MW m^{-2} compared with 6.7 MW m^{-2}. Many of the "nuclear physics" parameters, e.g. plasma pressure ratios and confinement time, are little different in the II-A and II-B reactors.

From the point of view of parametric studies of coolant circuits perhaps the main difference between the two reactors is that in the II-A, the pipes carrying coolant to and from the reactor run beside each other whereas in the II-B they are in a concentric arrangement; the hot helium from the reactor runs in a pipe within that carrying the cooler helium from the steam raising plant back to the reactor. In the former arrangement the stress in each pipe is due to the pressure difference between the inside (probably $\sim$ 60 bar) and the outside ($\sim$1 bar). In the concentric arrangement the stress for the cooler, outer, pipe is unchanged whereas for the inner one, which is hotter and has a considerably lower yield stress, the stress is now due only to the pressure drop within the reactor (not more than about 2 bar).

A concentric geometry will be used if the advantage of the reduced stress on the inner pipe outweighs the extra complexity in construction, control and maintenance (especially at times when the segements are removed for renewal (Mitchell, 1978; Mitchell and Hollis, 1976)).

It is the objective of this work to extend the earlier studies of coolant flow to elucidate the effects of using the concentric arrangement. Following the pattern of the previous work we first identify suitable pressure drop correlations for the junctions, then examine the flow in a row of blanket cells and finally consider a complete half segment.

2. PRESSURE DROP CHARACTERISTICS OF JUNCTIONS

In order to study the flow distribution in a concentric geometry it is first necessary to ascertain the pressure drop characteristics of the diverging and joining T's in the outer duct (the supply side) of a concentric network. The measurements are described by Shock (1983) and the conclusions and derived correlations relevant to this study are summarised in Appendix 1.

The changes to the computer program described by Shock (1979) for the implementation of the different geometry are fairly small. The pressure drop characteristics themselves were modified as described in Appendix 1 and the only other change is one needed so that for a given junction in the inlet flow (the outer pipe) the program can identify the size of both pipes in order to calculate the appropriate velocity. This is done by ensuring that the order of numbering the nodes on the outer pipe is the same as that on the inner. Corresponding pipes, one inside the other, then have a constant difference of node number (equal to half the total number of nodes). For a given pipe on the supply side, the diameter of the internal pipe can then be easily located.

3. BLANKET CELL ROW

In this section we repeat the earlier calculation for the five-cell row taking into account the concentricity. The geometry is illustrated in Figure 2. Note that it appears that the concentricity is maintained to within the inside of the blanket cell. With the basic concept proposed by Mitchell and Booth (1973) and used in the rest of this work, this cannot in practice be the case. The concept envisaged by Briaris and Stanbridge (1978), however, does have the concentricity maintained until within the blanket cells.

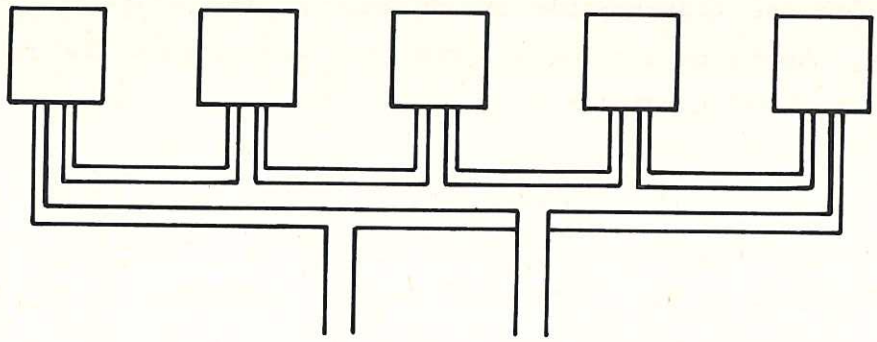

Fig.2 Arrangement for a five-cell row with concentric ducts.

It has been one objective of this work that it should differ from the previous only in the arrangement of the ducts. It should, however, be noted that one consideration has been omitted from all the blanket cell calculations carried out by any authors is the fact that the gas will accelerate

during its passage through the blanket cells, since the density will decrease. The extra pressure drop is estimated to be 10650 N m^{-2}. Some at least of this pressure drop will be recoverable as the gas decelerates during its passage in the steam raising plant. We have also not considered the pressure changes at the changes in section made at branches in the half segment ducting which keep the velocity constant. The irreverible changes at these sections in both supply and return ducting will be small.

The calculations carried out with the side-by-side arrangement were done for a standard set of conditions:

Coolant inlet temperature	= 300°C
Coolant outlet temperature	= 630°C
Cell internal ducting diameter	= 20 mm
Structure fraction	= 0.04
Wall loading	= 4.7 MW m^{-2}

The pressure drop and flow distribution were calculated for a range of duct diameters on the supply and removal sides. The calculations have been repeated here for the same duct sizes for the inner, coolant removal ducting and corresponding outer duct sizes. These latter ducts can be chosen to correspond in two ways; either the equivalent hydraulic diameter should be the same as for the side-by-side arrangement or the cross-sectional area, i.e. velocity, should be the same. Tables 1 and 2 show the results from these two modes of calculation.

In Table 1 D_s is the diameter of the outer, supply duct and $(D_e)_s$ is the equivalent hydraulic diameter of the annular channel in this flow - these are identical to the corresponding duct diameters in Table A1.1 of Shock (1979). K is the pumping power fraction for the five-cell row and, for comparison, K' is the corresponding value for the equivalent side-by-side arrangement. Finally M is the flow maldistribution defined by Shock (1979) to be

$$M = \left[\sum \left(\frac{W}{W_p} - 1\right)^2 \times \frac{1}{n_c}\right]^{\frac{1}{2}} \qquad (1)$$

M is zero if the flow of coolant is evenly distributed between the cells in a row and if, for example, the ratios of actual/desired flow for the cells, in order, are 1.25, 0.75, 0.75, 0.75, 1.25 then M = 0.3. In this case the

TABLE 1

Calculated Performance for a Five-Cell Row:

Equivalent Hydraulic Diameters as in Shock (1979)

D_s/m	$(D_e)_s$/m	D_r	Δp/bar	K	K'	M
0.10	0.05	0.05	18.0	0.268	0.268	0.270
0.125	0.075	0.05	17.8	0.264	0.250	0.310
0.15	0.10	0.05	17.7	0.263	0.247	0.323
0.125	0.05	0.075	4.13	0.061	0.074	0.086
0.15	0.075	0.075	4.02	0.059	0.059	0.104
0.175	0.10	0.075	3.99	0.059	0.057	0.110
0.15	0.05	0.10	1.88	0.028	0.044	0.030
0.175	0.075	0.10	1.81	0.027	0.029	0.038
0.20	0.10	0.10	1.79	0.026	0.026	0.041
0.30	0.20	0.10	1.78	0.026	0.025	0.039
0.25	0.05	0.20	0.87	0.013	0.030	0.004
0.30	0.10	0.20	0.85	0.013	0.013	0.002
0.40	0.20	0.20	0.84	0.012	0.012	0.003
0.325	0.075	0.25	0.81	0.012	0.015	0.001
0.45	0.20	0.25	0.80	0.012	0.012	0.001
0.5	0.25	0.25	0.80	0.012	0.012	0.001

TABLE 2

Calculated Performance for a Five-Cell Row:

Velocities as in Shock (1979)

D_s/m	D'_s/m	D_r	Δp/bar	K	K'	M
0.07	0.05	0.05	21.5	0.328	0.268	0.111
0.09	0.075	0.05	18.3	0.278	0.250	0.231
0.11	0.10	0.05	17.9	0.265	0.247	0.295
0.09	0.05	0.075	6.99	0.106	0.074	0.166
0.11	0.075	0.075	4.49	0.067	0.059	0.059
0.12	0.10	0.075	4.12	0.061	0.057	0.086
0.11	0.05	0.10	4.67	0.071	0.044	0.172
0.12	0.075	0.10	2.30	0.034	0.029	0.057
0.14	0.10	0.10	1.93	0.029	0.026	0.027
0.22	0.20	0.10	1.79	0.026	0.025	0.042
0.20	0.05	0.20	4.71	0.076	0.030	0.152
0.22	0.10	0.20	1.00	0.015	0.013	0.026
0.28	0.20	0.20	0.85	0.013	0.012	0.002
0.26	0.075	0.25	1.29	0.019	0.015	0.064
0.32	0.20	0.25	0.81	0.012	0.012	0.001
0.35	0.25	0.25	0.81	0.012	0.012	0.001

central cells would be starved of coolant and the outer pair overcooled.

In Table 2 the columns are identical except that D_s' (equal in value to the corresponding entry in Table 1) is now the duct diameter which would give the same velocities in a side-by-side arrangement.

The effect of changing the geometric arrangement is best seen from Figure 3 on which these data have been shown for comparison. The vertical axis shows the pumping power fraction and the horizontal axis shows D_s for the side by side arrangement, $(D_e)_s$, when we are considering the same equivalent hydraulic diameter and D_s' when we are considering the same velocity. Curves are drawn for two different values of D_r, about which there is no ambiguity.

The following conclusions can be drawn:

(i) For large supply ducts there is little difference between any of the K values, however calculated. This is not surprising since, for large external ducts, the pressure drop becomes dominated by the flow in the blanket cells, and in the return ducting whose size is constant for either group of curves. Figure 3 also shows the value of K for a single cell and indeed for large D_r and D_s the data for the five-cell row are asymptotic to this value.

(ii) For the same equivalent hydraulic diameter K is, at low D_s, less than the value for the side-by-side arrangement. Thus the effect of the reduced velocities (the available <u>area</u> is increased) offsets increased numbers of velocity heads at the junctions.

(iii) For the same velocity there is an increase of K at low D_s due to the increased numbers of velocity heads.

In the earlier studies the working values of D_r and D_s were chosen by determining that the value of K in the row should be 1.2 times that of a single blanket cell. The exact choice of the optimum D_r and D_s is a matter of trial and error since they are interdependent. In the earlier work the conclusion was drawn that $D_r = 0.17$. Making the same assumption here, Figure 4 is correspondingly drawn for several values of D_s and for $D_r = 0.2$.

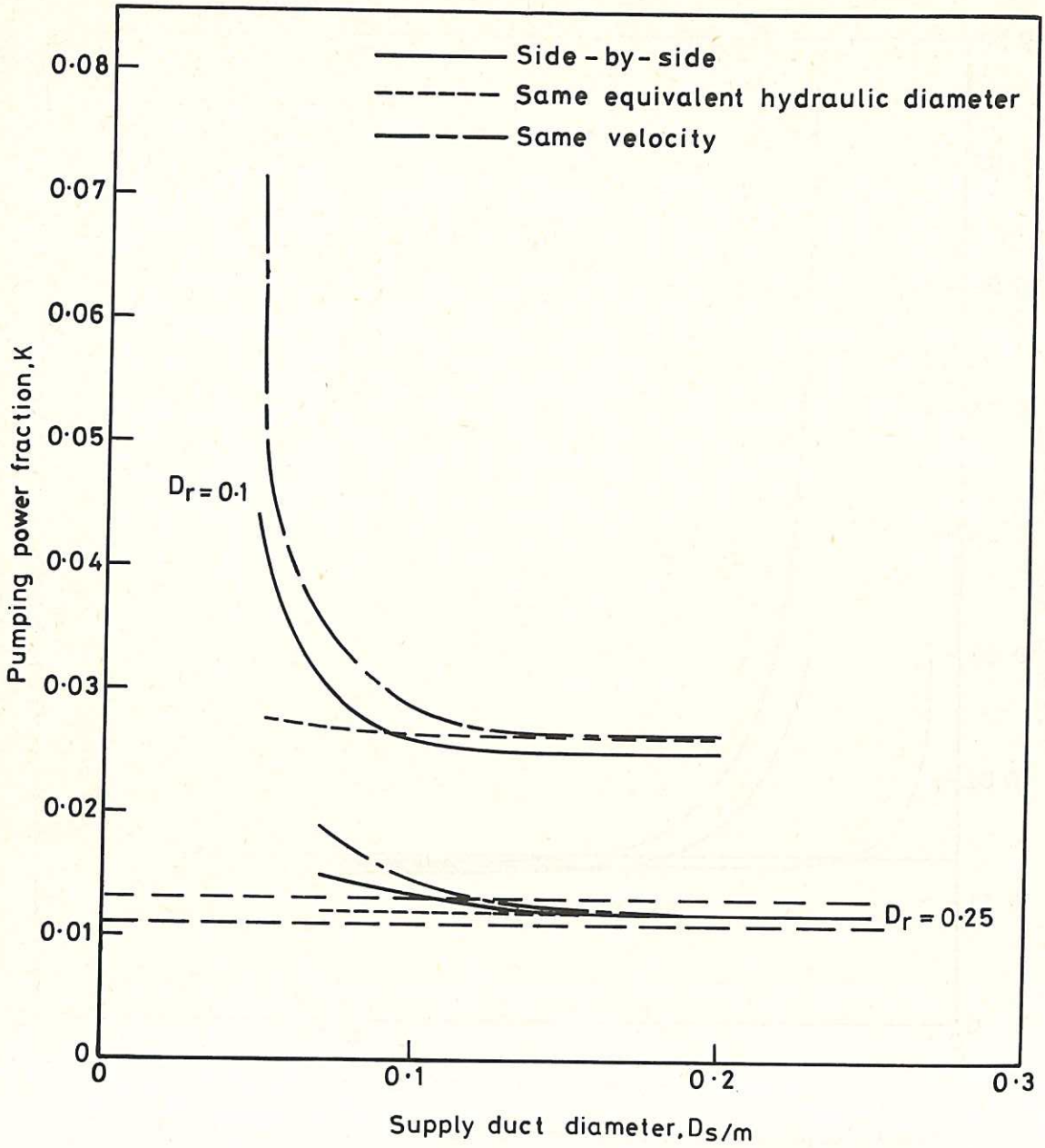

Fig.3 Pumping Power fraction for concentric ducting of a five-cell row: D_r = 0.1 and 0.25.

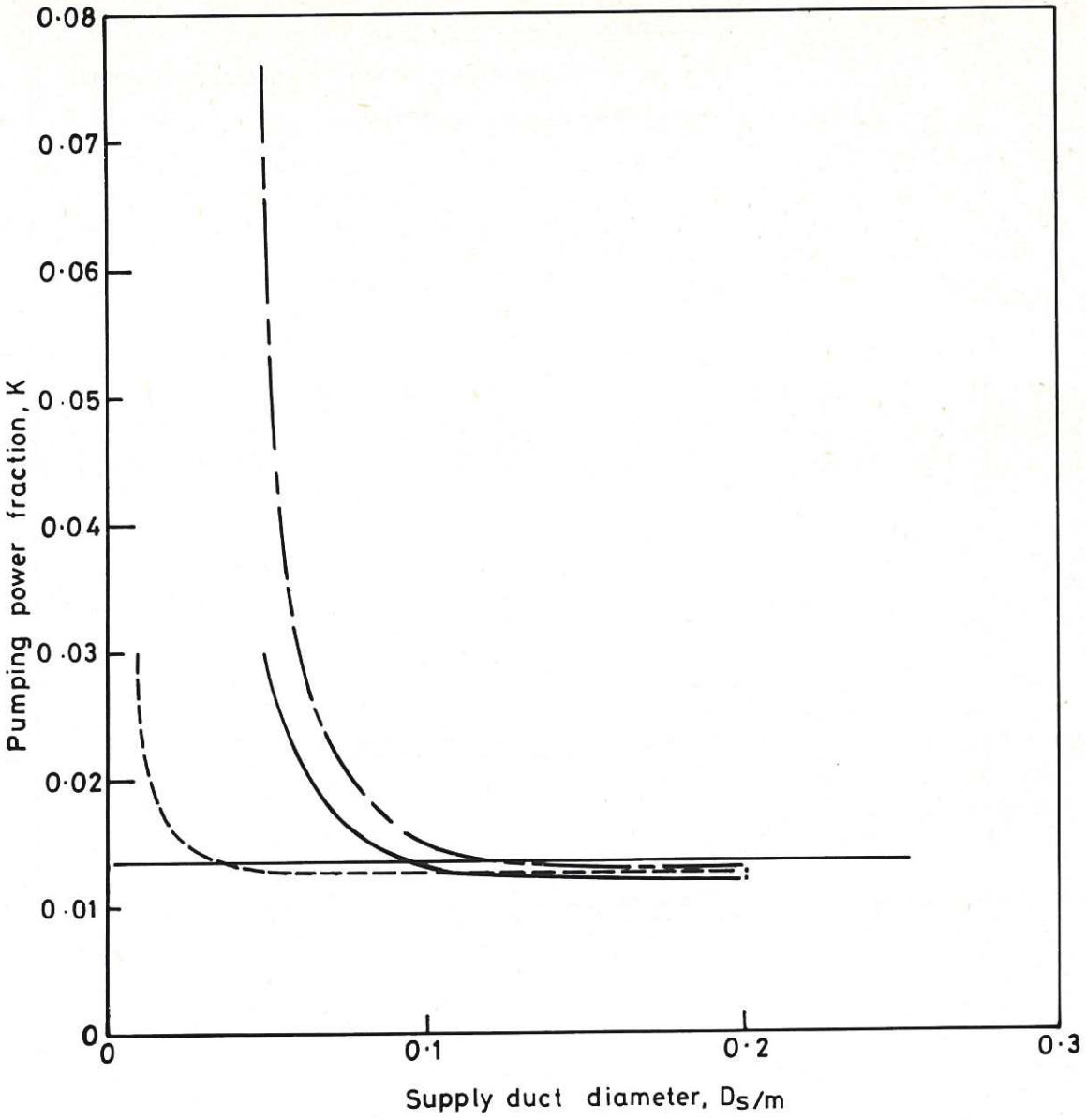

Fig.4 Pumping Power fraction for concentric ducting of a five-cell row: $D_r = 0.2$.

For K = 0.135 we then find that the minimum duct diameter on the supply side must be 0.036 m when the calculations are done on the basis of the same equivalent hydraulic diameter and 0.12 m for the same velocity. For the former case the actual diameter of the outer pipe (to give D_e = 0.036 m) is 0.23 m (ignoring the thickness of the inner pipe). For the latter case the actual diameter of the outer pipe (to give the same area as a round tube of diameter 0.12 m) is also calculated to be 0.23 m. The maldistribution is 0.02, which is probably a satisfactorily low value.

It should be no surprise that these values are the same since the two curves for the concentric geometry are calculated from the same computer program with merely a different set of values of diameter of the outer pipe. Nevertheless some interesting points can be made in carrying out the calculations on the two different bases as above.

The mean hydraulic diameter, 0.036 m, can be compared with the 0.12 m (for a D_r of 0.17 m) found with the side-by-side arrangement. Perhaps a better comparison is that the velocity of the full gas flow is now 52 ms^{-1} compared with 67 ms^{-1} for the side-by-side arrangement. In other words the extra head loss at the junctions is dictating a requirement for lower velocities in order to meet the overall pumping power fraction.

Use of the concentric arrangement with the above size means that the proportion of the cross-sectional area at the back of a blanket cell covered by the projection of the cooling manifold serving a row is now 45% compared with 57% for the side-by-side arrangement (in each case ignoring pipe and lagging thicknesses). This reduction in the space taken up by coolant ducting offers advantages with respect to the siting of the many other pieces of ancillary equipment both concerned with the plasma, e.g. divertors and injectors, etc., and with the blanket cells, lithium and tritium handling.

4. HALF SEGMENTS AND COMPLETE COOLING CIRCUIT

This section considers the ducting which supplies the coolant to the blanket cell rows and in turn feeds the exit hot gas to the steam raising equipment and recirculating compressors.

We first investigate the range of possible sizes for the ducts carrying the entire coolant flow to and from a half segment, that is before they

bifurcate to feed the rows of blanket cells. The geometry considered is shown in Figure 5. The return ducting carrying the hot gas from the reactor is of diameter D'_r and of wall thickness t_i. Since the inner and outer pipes, probably to be constructed of stainless steel, are carrying gas at high velocities (to reduce the size) and at temperatures separated by up to 400°C the transfer of heat between the two, although highly undesirable, would occur at a rapid rate were it not for the lagging of thickness l_i. This is shown, rather arbitrarily, as being on the outside of the return duct. If this were to be one of the current lagging media it would have to be very securely bonded to the pipes - perhaps the material and fastening used in the U.S. space shuttle could be employed. Other possibilities are to coat the outside of the return duct with a non-conducting ceramic material or even to make the duct itself out of such material. For the present study, however, we consider the system shown in Figure 5. The inner diameter of the outer, supply, duct is $(D'_s)_i$ and it is of thickness t_o and surrounded by lagging of thickness l_o. The width across the annular gap of the supply duct is S_s.

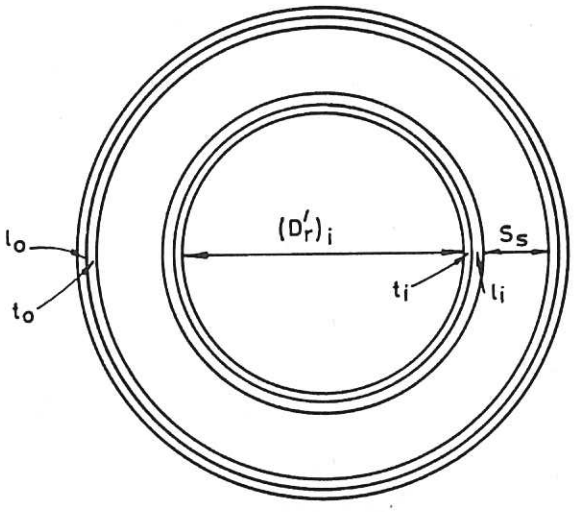

Fig.5 Concentric ducting showing lagging and tube walls.

As before (Shock, 1979, 1980) we argue that the space taken up by the piping plus a suitable gap, G, to allow room for remote cutting and welding should be no more than the outer width of the half segment.

The width of the half segment in CCTR-II-B is 2.65 m, at the outermost point. Hence

$$2\,l_o + 2\,t_o + 2\,S_s + 2\,l_i + 2\,t_i + (D'_r)_i + G = 2.65 \qquad (2)$$

As before we allow l_o to be 50 mm and G to be 0.2 m. The outer diameter of the supply pipe $(D'_s)_o$ is given as

$$(D'_s)_o = 2.65 - G - 2\,l_o \qquad (3)$$

which is thus 2.35 m. We can now apply the Lamé equation

$$(D'_s)_i = (D'_s)_o \sqrt{\frac{f - p}{f + p}} \qquad (4)$$

to give the value of $(D'_s)_i$ for $(D'_s)_o = 2.35$ and for various allowable stresses f and pressures p. The allowable stresses are taken from Figure 5 of Shock (1979) assuming a gas inlet temperature of 300°C and are as follows:

TZM : f_{300} = 380 MPa
Inconel 718 : f_{300} = 240 MPa
Stainless steel 316 : f_{300} = 55 MPa

The corresponding values of $(D'_s)_i$ are shown in Table 3 below.

TABLE 3

Coolant Duct Sizes Limited by Strength and Space Considerations

Material	Pressure/bar	$(D'_s)_i$/m
TZM/Inconel	0	2.35/2.35
	20	2.34/2.33
	40	2.32/2.31
	60	2.31/2.29
Stainless Steel 316	0	2.35
	20	2.26
	40	2.18
	60	2.11

Note the small difference between the data for $(D'_s)_i$ for TZM and Inconel 718. If TZM or Inconel are used t_o is only about 3 cm, whereas for stainless steel it is 12 cm. Current technology is for pipe sizes to be

available up to about 60" - so in view of the probable timescale involved the possible extrapolation required is not too great.

The next step in the procedure is to evaluate S_s and D'_r. Calculation shows that a lagging thickness of about 1 cm, with thermal conductivity about that of conventional lagging (say 0.2 W m^{-1} K^{-1}) will be sufficient to limit the heat transferred between the hot and cold streams to less than 1/10 of one percent of the total energy production. Thus we take l_i = 1 cm.

With respect to t_i, little mechanical strength is required because the pressure difference across this pipe will be small. Currently for common pipe sizes, up to about 0.3 m, the ratio of outside to inside diameter is about 1.05. This would imply t_i = 2.5 cm - which seems reasonable.

The areas of the ducts are calculated now on the assumption that the velocity of the gas should be identical in each pipe. The mass flow in the main supply duct is given by

$$W = n_s P_w A_w / C_p \Delta T \qquad (5)$$

and the necessary duct area, for a given velocity, is given by

$$A = \frac{W}{\rho U} \qquad (6)$$

From equations (2), (5) and (6) we can calculate the values of S_s and $(D'_r)_i$ which give the same velocity in the supply and return ducts for various values of W, using the values of n_s, A_w and ΔT appropriate to CCTR-II-B. These values of W thus correspond to various wall loadings; P_w = 4.7 MW m^{-2} is the current value for CCTR-II-B. The values of ρ, in the supply and return ducts, are taken to be those corresponding to various arbitrary pressures, see Table 4, and temperatures of 300°C and 630°C respectively.

Values of S_s and $(D'_r)_i$, shown in Table 4, have been calculated for a velocity of 60 ms^{-1}. This is about the maximum currently envisaged and imposes the lower limit of tube size. Table 4 also shows the corresponding inside diameter of the outer supply duct; the outside diameter will vary slightly with the material.

TABLE 4

Duct Sizes for Various Flowrates and Pressures:

Velocity Set to 60 ms^{-1}

$W/(kg\ s^{-1})$	$P_w/MW\ m^{-2}$	p/bar	$(D'_r)_i/m$	S_s/m	$(D'_s)_i/m$
100	9.9	5	2.81	0.30	3.55
		10	1.98	0.21	2.55
		20	1.40	0.14	1.84
		40	0.99	0.10	1.33
		60	0.81	0.079	1.12
47.5	4.7	5	1.93	0.20	2.49
		10	1.37	0.14	1.80
		20	0.97	0.096	1.31
		40	0.68	0.065	0.96
		60	0.56	0.051	0.81
20	2.0	5	1.25	0.128	1.66
		10	0.89	0.087	1.21
		20	0.63	0.059	0.89
		40	0.44	0.039	0.67
		60	0.36	0.030	0.57

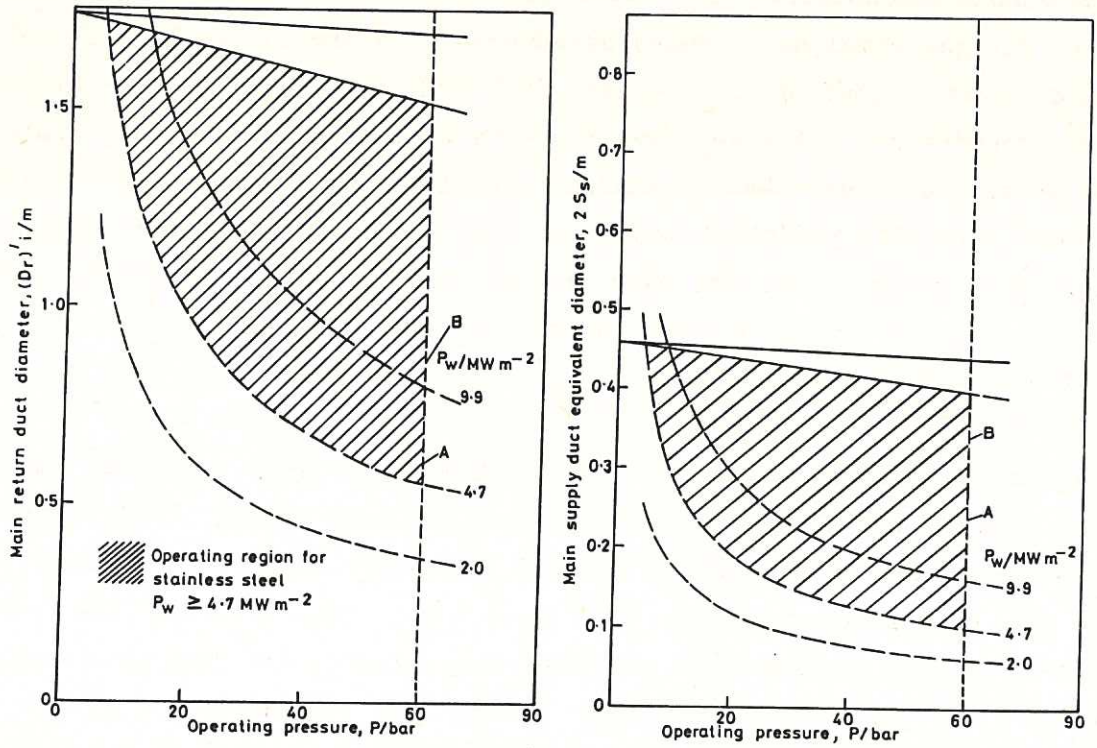

Fig.6 Size limitation of main cooling ducts. The curved lines show the minimum duct diameter versus pressure for three values of wall loading, P_w.

These figures for minimum duct size are plotted in Figure 6 together with those for maximum size based on the value of $(D'_s)_i$ from Table 3 and the, rather arbitrary, assumption that the velocities in the two ducts should be equal (thus allowing for the change in density). The dotted line in the graph for 2 S_s is the equivalent value for the case when the areas are equal (not thus allowing for the change in density). The value of 2 S_s is used because this is a close approximation to the equivalent hydraulic diameter. A closed operating region is set by imposing a maximum pressure of 60 bar set by current compressor limitations.

As in the earlier work we choose a base case within this region for CCTR-II-B (i.e. P_w = 4.7 MW m^{-2}) where the pressure is 60 bar and the velocity in the return ducts is 50 ms^{-1} and is 30 ms^{-1} in the supply ducts. The corresponding sizes $(D'_r)_i$ = 0.61 m and S_s = 0.12 m are marked A in Figure 6; for stainless steel this would mean that the outer tube would be of inside diameter 0.91 m and outside diameter 1.02 m and for TZM and Inconel the outside diameter would be 0.93 m.

Clearly, in practice, the pipe sizes would be chosen according to available standard dimensions. The sizes quoted above are well within current practice for gas pipelines. Round-edged equal T's are currently available in standard sizes including 24, 30 and 36" and of the required thickness. Although round-edged T's give lower pressure drop they require more space due to the gentle curvature than do sharper junctions and it is considered likely that sharp, welded, junctions would be used on fusion reactors; appropriate pressure drop correlations are used throughout this work. It should also be noted that a sound system of location of the inner pipe within the outer must be devised.

Having decided on a base set of sizes for the pipes carrying the main coolant flow we now follow the system used earlier (Shock, 1979, 1980) and fix a standard set of dimensions for all the other inter-cell ducting. The sizes are calculated assuming that each cell row receives its correct proportion of the coolant flow and that the velocity is maintained constant at 50 ms^{-1} in the return duct and 30 ms^{-1} in the supply. It is also assumed that the ratio $(D'_s)_i/(D'_r)_i$ will remain constant at about 1.1. The pipe sizes calculated for these conditions are shown in Figure 7. It is encouraging to note that these result in the conclusion that the sizes of the pipes feeding the five-cell rows $(D'_r)_i$ = 0.17 m and

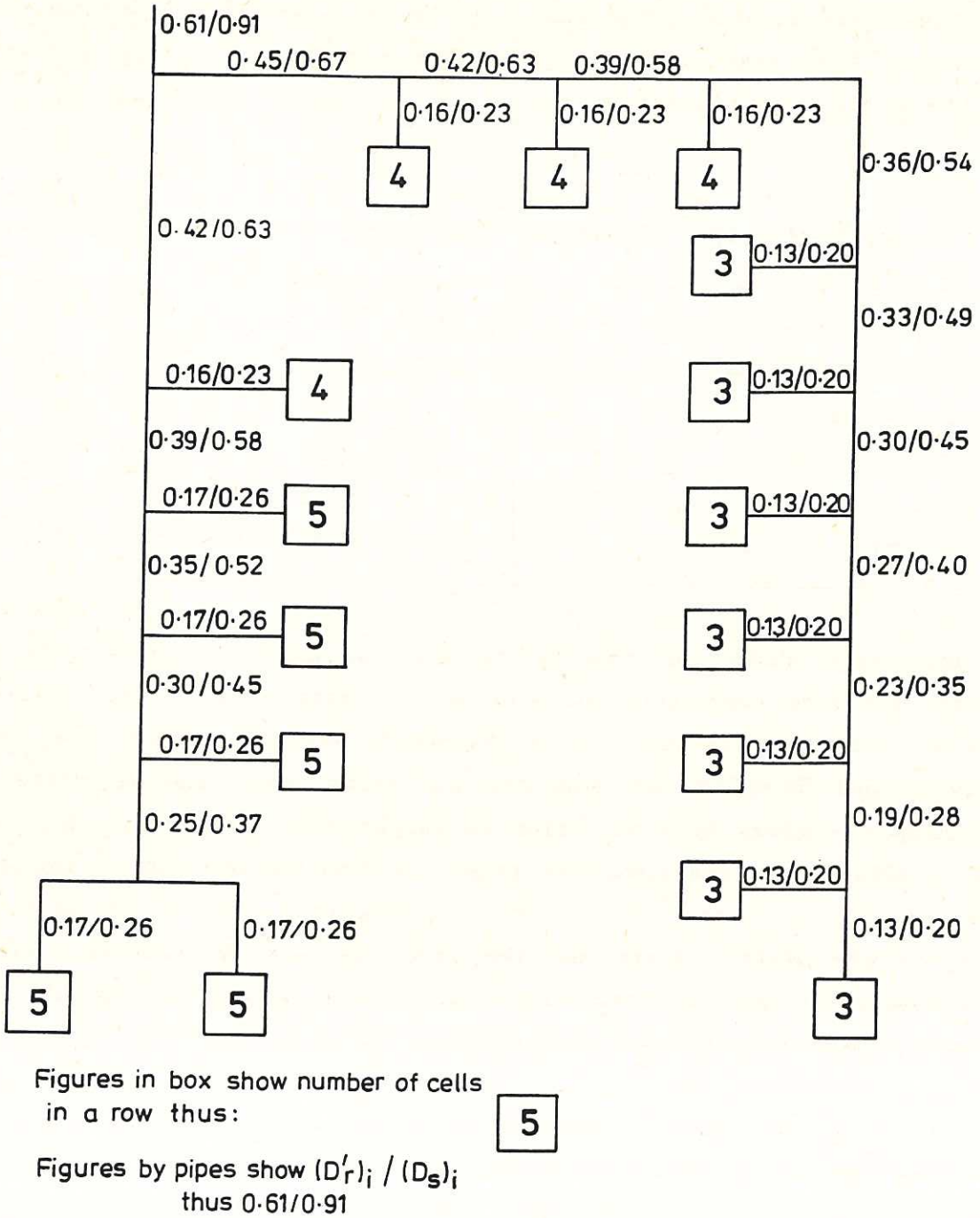

Fig.7 Standard geometry for half segment.

$(D'_s)_o$ = 0.26 m are very close to those calculated, from different criteria, in the previous section.

With these 'standard' pipe sizes the pressure drop for this geometry is 1.01 bar and M = 0.0007. These data are compared in Table 5 with values for the side-by-side arrangement.

TABLE 5

Performance of Complete Half Segments: Standard Geometry

Arrangement	Δp/bar	K	$K_{overall}$	M
Concentric	1.013	0.0166	0.0235	0.0007
Side-by-side	1.011	0.0166	0.0235	0.034
Concentric (all v = 50 ms^{-1})	1.19	0.0195	0.0266	0.037
Side-by-side (all v = 50 ms^{-1})	1.10	0.0181	0.0251	0.041

The table shows the results of the calculations for the standard geometry for both concentric and side-by-side arrangements (where the duct sizes are such that the velocity in the supply and return ducts are respectively 30 and 50 ms^{-1}) and also for the cases where the velocities are both 50 ms^{-1} - given by a reduction is supply side duct size. The values of K, pumping power fraction, are those for the complete half segment and those of $K_{overall}$ are those for the complete circuit including the piping to the steam raisers and the steam raisers themselves. This is calculated following the assumptions made by Shock (1979) that the extra pressure drop is 0.35 bar and the compressor efficiency is 0.95.

We can see in Table 5 that the concentric arrangement imposes a very small increase in pressure drop for the 30/50 ms^{-1} sizes but that the maldistribution is much smaller (note that it is small anyway even for the side-by-side arrangement). The change in pressure as we follow the gas through the ducting to and from one of the cell rows is illustrated in Figure 8. We can see that, for this particular case, the extra head loss in the dividing T (from junction 4 to 5) means that less gas follows this path and the oversupply, present in the side-by-side arrangement, is partially corrected; hence the reduction in maldistribution.

The difference in pressure drop is somewhat more marked for the case where the velocities are each 50 ms^{-1} and we can conclude from the results that the pressure drop in the concentric arrangement is more

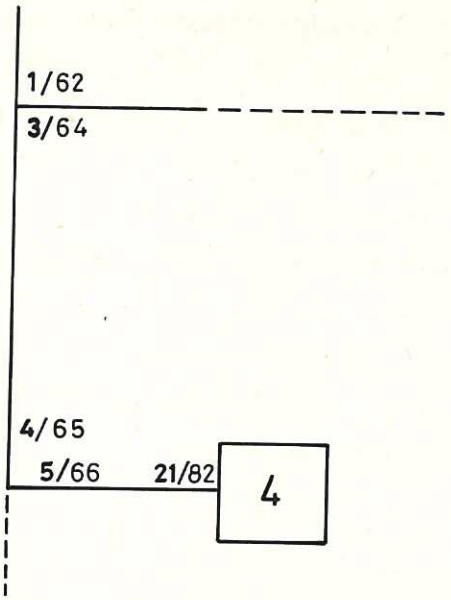

Figures in bold type are node points on supply side
Figures in light type are node points on return side

Flow path	Pressure charge $(P_{upstream} - P_{downstream})$	
	Side-by-side	Concentric
1 ↓ 3	− 403	− 172
3 ↓ 4	+ 44	+ 164
4 ↓ 5	+ 791	+ 6731
5 ↓ 21	+ 248	+ 1136
21 ↓ 82	+ 95863	+ 89540
82 ↓ 66	+ 398	+ 357
66 ↓ 65	− 174	− 762
65 ↓ 64	+ 70	+ 93
64 ↓ 62	+ 4324	+ 4248
Overall $\Delta p / Nm^{-2}$	101161	101325

Fig.8 Pressure drop distribution in one flowpath through a segment.

sensitive to flow velocities than in the side-by-side pattern.

In the previous parametric study a series of runs was carried out with the basic geometry and a series of curves was plotted giving overall K as a function of the coolant flowrate per cell. Figure 9 shows the results obtained. Repetition of these runs shows negligible deviation from these results, although the maldistributions are smaller. Thus the operating envelopes based on these lines drawn by considerations of minimum economic wall loading and thermodynamic efficiency and maximum surface temperature and pumping power fraction are not effectively altered.

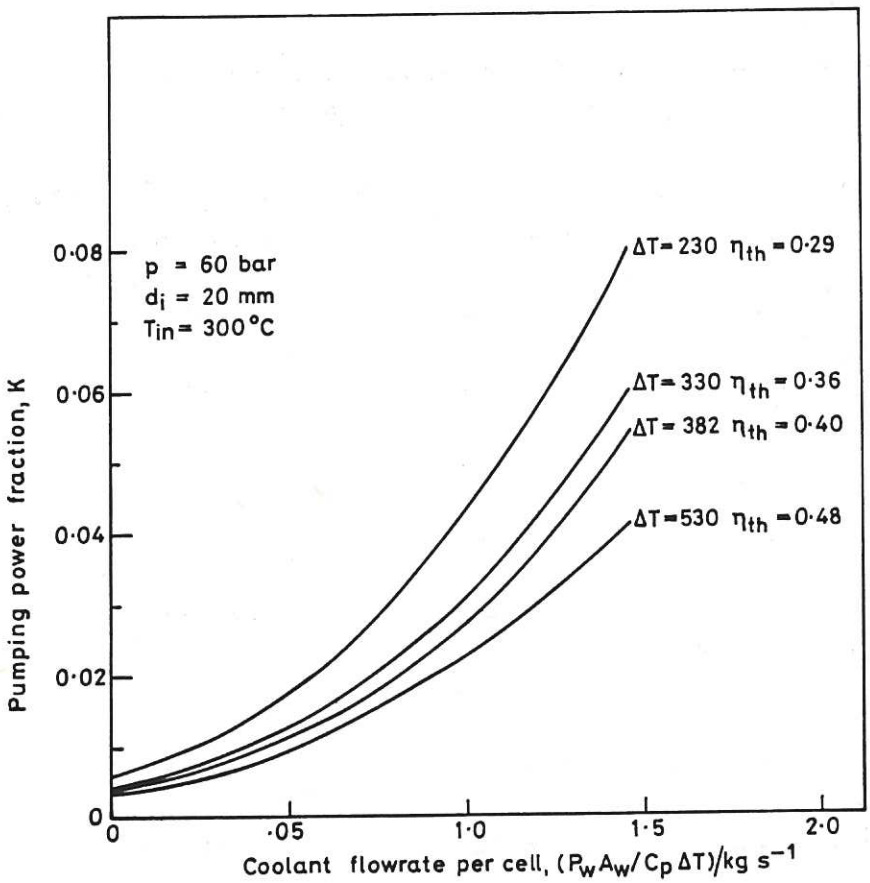

Fig.9 Plot of overall pumping power fraction against coolant flow rate for various thermodynamic efficiencies, for the case of side-by-side ducting.

So far the ducting arrangement has been assumed to be based on the half segment (in order to maintain similarity with the previous studies). In this case all the cell rows in the top or bottom half of one segment are cooled by a common main manifold and operate a single steam raiser.

Following the details of the arrangement for CCTR-II-B, however, it is more likely that it will be a complete segment which will be commonly ducted. Calculations have thus been done on this basis for the standard set of conditions. Duct sizes have again been chosen so that the inlet and outlet velocities are 30 and 50 ms^{-1}. The corresponding main supply and removal duct sizes are shown as B on Figure 6. The overall pressure drop for the complete segment is 104800 N m^{-2} and the maldistribution 0.078, compare the 101300 N m^{-2} and 0.0007 for the half segment.

5. DISCUSSION AND CONCLUSIONS

The general effect of changing to a concentric geometry appears to be, in general, a slight increase in pressure drop for the cell rows and a negligible increase for the complete half segment. In the latter case the maldistribution is, however, greatly reduced.

The advantages of using the concentric geometry are twofold. Firstly the large material saving on the hot duct side and secondly the saving in space. As for the cell row, the projected area occupied by pipe (and lagging, etc.) is decreased; for the segment it changes from 53% to 38% - again leaving more room for injectors and divertors.

The disadvantages lie mainly in the increased complexity, and therefore expense, both of the initial construction and the equipment for remote cutting and handling during first wall replacement operations. Some thought will have to be given to the way in which the inner tube is to be supported in the outer. In the experiments described by Shock (1982) the inner tube was supported by three pins placed systematically around the axis. Some thought will have to be given to the possibility that the gas flows and tubes could interact and cause the inner tube to vibrate - it is estimated, however (Goyder, 1982), that this is not likely to be a major problem.

NOMENCLATURE

A	Duct cross sectional area	m^2
A_w	Front wall area of cell	m^2
C_p	Specific heat capacity	$J\ kg^{-1}\ K^{-1}$
D	Diameter	m
D_e	Equivalent hydraulic diameter	m
f	Maximum allowable stress	$N\ m^{-2}$
g	Acceleration due to gravity	$m\ s^{-2}$
G	Gap between main coolant pipes	m
K	Pumping power fraction	-
K'	K for side-by-side geometry	-
l	Length of pipe, lagging thickness	m
M	Maldistribution	-
n_c	Number of blanket cells per row	-
n_s	Number of blanket cells per half segment	-
p	Pressure	$N\ m^{-2}$
P_w	Wall loading	$N\ m^{-2}$
S	Annular gap	m
t	Wall thickness	m
T	Temperature	K
U	Velocity	$m\ s^{-1}$
W	Flowrate	$kg\ s^{-1}$
W_p	Ideal flowrate for zero maldistribution	$kg\ s^{-1}$
x_b	Ratio of branch to total flow at a junction	-
ξ	Number of velocity heads lost at a junction	-
ρ	Density	$kg\ m^{-3}$
ψ	Friction factor	-

Subscripts

B	Branch
D	Downstream
i	Inside
o	Outside
r	Return
s	Supply
U	Upstream

Superscript

'	Main segment ducting

REFERENCES

BRIARIS, D.A. and STANBRIDGE, J.R. (1978) Design of the segment structure and coolant ducts for a fusion reactor blanket and shield. Culham Laboratory Report No. CLM R 184.

GOYDER, H.G.D. (1982) Private Communication.

GUTHRIE, J.A.S. and HARDING, N.H. (1981) Culham Conceptual Tokamak Mark II design study of the layout of a twin-reactor fusion power station. Culham Laboratory Report No.CLM R 215.

IDEL'CHIK, I.E. (1966) Handbook of Hydraulic Resistance. Coefficient of local resistance and of friction. UKAEC Report No. AEC-TR-6630.

KAY, J.M. (1965) An Introduction to Fluid Mechanics and Heat Transfer. 2nd Ed., Pub. Camb. Univ. Press.

MILLER, D.S. (1971) Internal Flow. A guide to losses in pipe and duct systems. BHRA, Cranfield, Bedford.

MITCHELL, J.T.D. (1978) Blanket replacement in Toroidal fusion reactors. ANS, 3rd Topical Meeting on Technology of controlled nuclear fusion, Santa Fe, Mexico.

MITCHELL, J.T.D. and HOLLIS, A. A Tokamak reactor with servicing capability. FTSG/76/89.

SHOCK, R.A.W. (1979) Helium cooling circuits for a fusion reactor. Culham Laboratory Report No.CLM P 572.

SHOCK, R.A.W. (1980) Helium cooling circuits for a fusion reactor. Nucl. Eng. Des., 61, 277-294.

SHOCK, R.A.W. (1983) Pressure drop in T's in concentric ducts. AERE Report No. AERE-R 10673.

VAZSONYI, A. (1944) Pressure losses in elbows and duct branches. Trans. ASME, 66, 177-183.

A P P E N D I X 1

DERIVATION OF PRESSURE DROP RELATIONSHIPS

In this Appendix correlations are developed for the pressure drop characteristics of the junctions required for the reactor studies.

The studies carried out by Shock (1979, 1980) used pressure drop correlations derived by Vazsonyi (1944) for sharp-edged ducts. A brief examination of the data available in the literature for the pressure losses in T's in simple round tubes appears to show a great deal of scatter. There is, however, little doubt that much of this scatter is simply due to the fact that different workers have employed T's of different geometry (e.g. sharp or round-edged, screw fitting) and that this has a profound influence on the pressure drop characteristics. In relation to the studies described here the following general conclusions can be drawn.

(i) Miller (1971) carried out tests with both sharp and round-edged junctions.

(ii) His data for sharp-edged junctions are in reasonable agreement with the correlation of Vazsonyi (1944), used in the earlier studies by Shock (1979, 1980).

(iii) The data of Miller (1971) and Shock (1983) for round-edged junctions are in reasonable agreement.

This then gives confidence to the pressure drop for the entire cooling circuit estimated, for the case of sharp-edged junctions, by Shock (1979, 1980).

The experimental study on pressure drop characteristics has shown the effect of concentricity for a round-edged outer-tube with a square-edged insert. These measurements are applied in the main text to examine the effect, on Δp in CCTR-II-B, of using a concentric piping arrangement. It will be assumed that the effect of going from a round to a concentric tube arrangement (an increase of up to 0.3 velocity heads, see Appendix 2) is itself independent of the detailed shape of the junctions. Thus we assume that most of the extra pressure drop simply arises from the obstruction due

to the inner pipe. This assumption is sufficient for the purposes of this study but some more, fairly simple, work would be required if the concentric system were to be seriously pursued for power plant.

The correlations of Vazsonyi were in pressure drop explicit form and, for use in the reactor analysis, a multiplying factor of 1.25 was used to allow for the effect of neighbouring junctions. Thus, for example, for converging flow the pressure drop for the flow continuing along the manifold is given by

$$\Delta p = \frac{\rho}{1.6}\left[2\,U_D^2 - 0.05\,U_U^2 - 2\,U_D\left(0.205\,U_B\frac{W_B}{W} + U_U\frac{W_U}{W_D}\right)\right] \qquad \text{(A1.1)}$$

The types of fitting with which we are concerned are illustrated in Figure A1.1 (note, we evolve, for completeness, correlations for both joining and dividing T's although in the current geometry there are none of the former in the outer, annular, ducts).

The characteristics of the blanket cells are calculated as described in Section 2 of Shock (1979) and the relationships for the inner pipes of the concentric system are those given in Appendix 1 of Shock (1979) and illustrated in equation (A1.1).

For the outer pipe of a straight section of concentric ducting, we use the same equation as before

$$p_1 - p_2 = \frac{1}{2}\psi\,\rho\,U^2\,\frac{1}{D} \qquad \text{(A1.2)}$$

with D, the diameter, now replaced by D_e, the equivalent hydraulic diameter, given in this case by

$$D_e = D_o - D_i \qquad \text{(A1.3)}$$

where D_o is the diameter of the outer and D_i that of the inner pipe.

For dividing and converging flows Type 2 we evolve correlations from the following arguments based on the ideas given at the beginning of this section.

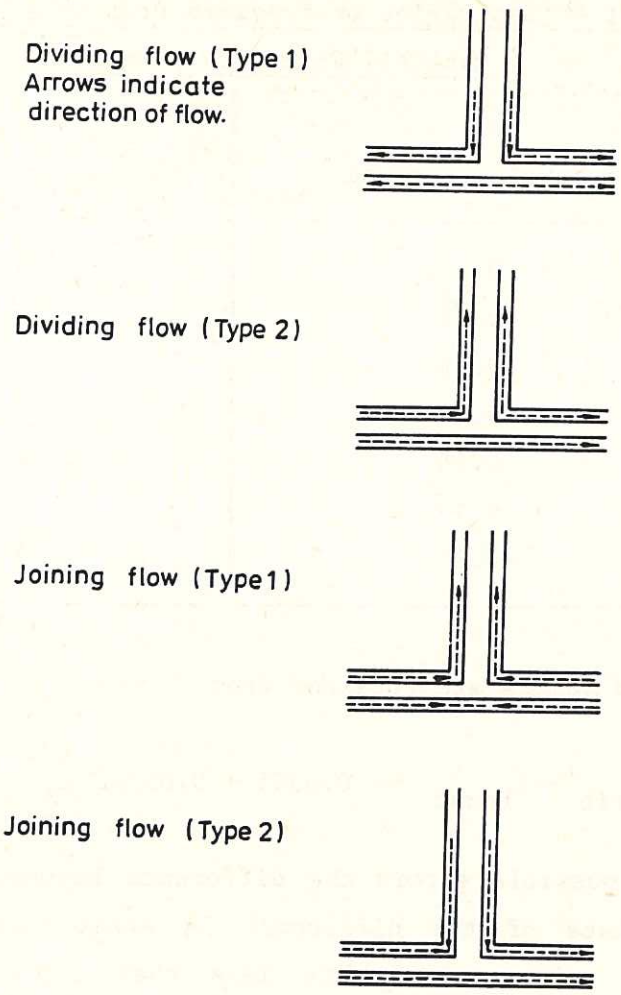

Fig.A.1 Configuration of dividing and joining flows in concentric ducts.

(i) Take the basic correlation of Vazsonyi for square-edged junctions, without the factor 1.25, and put it in ξ-explicit form. Thus, for the flow along the manifold in converging flow, equation (A1.1) is modified to give

$$\xi = 1 + 0.95 \left(\frac{U_U}{U_D} \right)^2 - \frac{2}{U_D} \left(0.205\, U_B \frac{W_B}{W_D} + U_U \frac{W_U}{W_D} \right) \qquad \text{(A1.4)}$$

(ii) Find, from the results of Shock (1983), the number of extra velocity heads due to the presence of the inner pipe. For the case being followed we can draw up the following table:-

TABLE A1.1

Effect of Inner Pipe on Pressure Drop in a Junction:

Manifold Flow for Joining T

x_b	$\left[\xi_{concentric} - \xi_{round}\right]_{exptl}$	$\left[\xi_{concentric} - \xi_{round}\right]_{calc}$
0.1	0.37	0.37
0.2	0.19	0.20
0.3	0.11	0.14
0.4	0.10	0.12
0.5	0.10	0.10
0.7	0.10	0.08
1.0	0.10	0.07

The calculated values are obtained from

$$\xi_{concentric} - \xi_{round} = 0.0325 + 0.03375/x_b \qquad (A1.5)$$

Noting other possible errors the difference between experimental and predicted values of the difference is small (anyway in a fusion reactor most values of x_b are less than 0.5). As $x_b \rightarrow 0$ the difference calculated by the formula is constrained within the following calculations to be $\leqslant 0.75$ (see Figure 17 of Shock, 1983).

For the other types of junction the numbers of extra velocity heads caused by the presence of the inner tube are as follows:

Converging flow, branch : 0.1 (see Figure 18, Shock, 1983)
Diverging flow, manifold : 0 (see Figure 19, Shock, 1983)
Diverging flow, branch : x_b for $x_b \leqslant 0.2$
0.2 for $x_b > 0.2$ (see Figure 20, Shock, 1983)

(iii) The total number of velocity heads lost is found by adding the contributions from steps (i) and (ii) above.

(iv) The calculated value of ξ is reconverted to a pressure drop and the factor 1.25 reintroduced.

For the junctions of type 1 the situation is somewhat more complex since they were not included in the original experiments; they are also found much less frequently in the manifolding networks although they do give proportionately higher pressure drop (certainly for converging flow).

Since no data are available it is necessary to make assumptions. For the divide, type 1, we are concerned with flow which is branching off a common line and simultaneously turning round a bend. The original correlation for simple round tubes with this configuration gives the pressure drop by the same formula as the branch flow in a type 2 divide. Since the dividing flow in each case is turning round a 90° bend we assume that the extra resistance due to the inner tube is also identical. Thus for the divide, type 1, we assume:

$$\xi_{\text{concentric}} - \xi_{\text{round}} = \begin{cases} x_b \text{ for } x_b \leq 0.2 \\ 0.2 \text{ for } x_b > 0.2 \end{cases}$$

where logically x_b must now be set to the proportion of the total flow travelling in the direction in question.

For the converging flow, type 1, we will similarly assume that the extra resistance due to the flow round the right angled bend is reasonably similar to that for the branch flow in a joining T of type 2, i.e.:

$$\xi_{\text{concentric}} - \xi_{\text{round}} = 0.1$$

In connection with assumptions made above it may be noted that in the experiments carried out the number of extra velocity heads lost for flow round the 90° bend in both dividing and converging systems was always in the range 0 to 0.2.

APPENDIX 2

THE MEANING OF VELOCITY HEAD

It can be shown (Kay, 1965) that in flow without irreversible losses (such as are imposed by wall friction and pipe fittings) the sum of terms

$$\frac{p}{\rho g} + \frac{U^2}{2g} + h = \frac{p_o}{\rho g} \qquad \text{(A2.1)}$$

(note, p is the static pressure, that measured by a pressure tapping flush with the wall of a duct) is constant. This extremely useful equation shows that, for example, in a horizontal system an increase in velocity (through a gradual decrease in available area) leads to a decrease in pressure; an aircraft wing is shaped so that there is an increase in velocity in the flow over the upper wing, the lift results from the decrease in pressure. The above terms all have the dimension of length and they are customarily referred to respectively as pressure head, velocity head, static head and total head.

Not only can the pressure change reversibly (e.g. in the above example the pressure will increase if the flow area is increased) but it can also change irreversibly through friction at the walls and losses in pipe fittings. In this case the total head will not be constant and it is customary in calculation of the pressure loss to express the change in total head in terms of numbers of velocity heads, i.e.

$$\frac{\Delta p_o}{\rho g} = \frac{\xi U^2}{2g} \qquad \text{(A2.2)}$$

$$\text{or} \quad \Delta p_o = \xi \frac{\rho U^2}{2} \qquad \text{(A2.3)}$$

where ξ, the number of velocity heads for a particular sort of fitting, can be found in appropriate compendia of data, e.g. Idel'chik (1966).

HER MAJESTY'S STATIONERY OFFICE

Government Bookshops

49 High Holborn, London WC1V 6HB
(London post orders: PO Box 569, London SC1 9NH)
13a Castle Street, Edinburgh EH2 3AR
Brazennose Street, Manchester M60 8AS
Southey House, Wine Street, Bristol BS1 2BQ
258 Broad Street, Birmingham B1 2HE
80 Chichester Street, Belfast BT1 4JY

Publications may also be ordered through any bookseller